EurJIC European Journal of Inorganic Chemistry

ChemPubSoc Europe

FULL PAPER

DOI:10.1002/ejic.201300661

Shape and Size Tunable Synthesis of Coordination Polymer $Mn_2W(CN)_8{\cdot}xH_2O$ Microcrystals through a Simple Solution Chemical Route

Guoxing Zhu,[a,b] Yunyun Xiao,[a] Xiaoping Shen,*[a,b] Qingjing Zhang,[a] and Aihua Yuan[c]

Keywords: Synthesis design / Crystal growth / Microcrystals / Tungsten / Manganese / Cyanides

By using a simple solution chemistry approach with polyvinyprrolidone (PVP) as a capping agent, $Mn_2W(CN)_8{\cdot}xH_2O$ microcrystals with unique morphologies including rice-like, rod, octahedron, square platelet, and hollow-core square platelet have been successfully synthesized. The influence of experimental parameters such as reaction temperature, feed ratio of Mn^{2+} to PVP, reaction time, and reactant concentration on the morphology and size of $Mn_2W(CN)_8{\cdot}xH_2O$ microcrystals were systematically investigated. The reaction temperature proved to be a key factor for morphological evolution of the products. It was found that 20, 55, and 85 °C were key points of morphological transformation. A possible growth mechanism of the $Mn_2W(CN)_8{\cdot}xH_2O$ microcrystals is proposed.

Introduction

In recent decades, intense research has been carried out on the synthesis of inorganic micro/nano-materials with various shapes, sizes and microstructures, because it is well-known that the properties of materials are closely related to the geometrical arrangement of the component parts.[1–4] However, studies on the control of microstructure and size for coordination polymers (CPs) are quite limited.[5] In fact, CPs have a number of merits as potential functional materials. For example, when used in functional devices, they often have better flexibility than more traditional inorganic materials.[6] The highly adjustable composition and structure due to the various organic ligands available and the diverse range of coordination interactions, provide CPs with high scope for developing and improving their functional properties. Scaling down these CP materials to micro-/nano-scale has afforded an exciting new class of highly tailored materials. Compared with bulk coordination polymers, promising micro-/nano-materials exhibit new possibilities to improve the intrinsic characteristics and develop novel shape- and size-dependent properties.[7]

In recent years, CP micro/nanocrystals composed of Prussian blue (PB) and its analogues have been prepared because of their simple and certain structure, and rich functionality.[8–12] Precise size and composition tailoring of PB analogue nanocrystals has been reported by Mallah's group.[13,14] Chen et al. demonstrated the fabrication of $M_3[Co(CN)_6]_2$ (M = Zn^{2+}, Cd^{2+}, Mn^{2+}, Co^{2+}) micro/nanostructures.[15–18] Patterning of PB-type nanoparticles and nanocomposites with various matrices were also obtained.[19–22] These PB and analogue micro/nanostructures show intriguing size- or shape-dependent magnetism,[23,24] optics,[25,26] gas storage,[17,18] and electrochemistry properties.[27,28] Despite the wide variety of morphologies and properties afforded by the PB family, little attention has been paid to micro/nanoscale objects made of octacyanometalate-based CPs. This is partly due to significant difficulties in their synthesis, because the complex molecular structure and changeful coordination modes cause uncertainty in the structures of the final CP products. Recently, interesting photomagnetic nanorods of $Cu_2Mo(CN)_8$ and photoinduced superparamagnetic nanoparticles of $CuNiMo(CN)_8$ have been synthesized by Catala et al.[29,26] Inspired by these pioneering reports,[30] we selected $Mn_2W(CN)_8{\cdot}xH_2O$ as a model compound to develop a shape- and size-tunable synthesis. As a typical octacyanometalate-based CP, $Mn_2W(CN)_8{\cdot}xH_2O$, with a three-dimensional network structure, crystallizes in a tetragonal system.[31] Its magnetic and porous properties were also reported in previous studies.[31] However, to the best of our knowledge, there is no report on the preparation of $Mn_2W(CN)_8{\cdot}xH_2O$ micro/nanocrystals.

In this report, we describe a simple aqueous solution method to prepare CP microcrystals from Mn^{II} and the

[a] School of Chemistry and Chemical Engineering, Jiangsu University,
Zhenjiang, 212013, China
E-mail: xiaopingshen@163.com
www.ujs.edu.cn
[b] School of Materials Science and Engineering, Jiangsu University,
Zhenjiang, 212013, China
[c] School of Biology and Chemical Engineering, Jiangsu University of Science and Technology,
Zhenjiang 212013, China

Supporting information for this article is available on the WWW under http://dx.doi.org/10.1002/ejic.201300661.

well-known octacyanometalate-based building block $[W(CN)_8]^{4-}$. The shape and size of the resulting $Mn_2W(CN)_8{\cdot}xH_2O$ microcrystals can be finely tuned with experimental parameters such as reaction temperature. Advantages of this method include easily controllable shape and size of the products, mild reaction conditions, and the use of water as the reaction medium. This preparation provides a convenient and environmentally friendly route to large-scale production of octacyanometalate-based CP microcrystals with tunable shape and size.

Results and Discussion

$Mn_2W(CN)_8$ microcrystals with different shape and size were prepared by a simple polyvinylpyrrolidone (PVP) assisted route. Mixing of a Mn^{2+} solution and a $[W(CN)_8]^{2-}$ solution led to a rapid color change from deep-yellow to light-yellow, suggesting the formation of $Mn_2W(CN)_8$. We initially investigated the preparation of $Mn_2W(CN)_8$ at a moderate temperature (65 °C), with [pyr]/[Mn^{2+}] = 100 (pyr = monomer vinylpyrrolidone). The phase structure of the as-synthesized product was first inspected by X-ray diffraction (XRD). The XRD pattern of the sample and the standard pattern of $Mn_2W(CN)_8{\cdot}xH_2O$ simulated from the single-crystal structure data are shown in Figure 1. It can be seen that all the diffraction peaks of the sample match well with those of the standard pattern, indicating that $Mn_2W(CN)_8{\cdot}xH_2O$ was successfully obtained by using the PVP-assistant aqueous solution route.

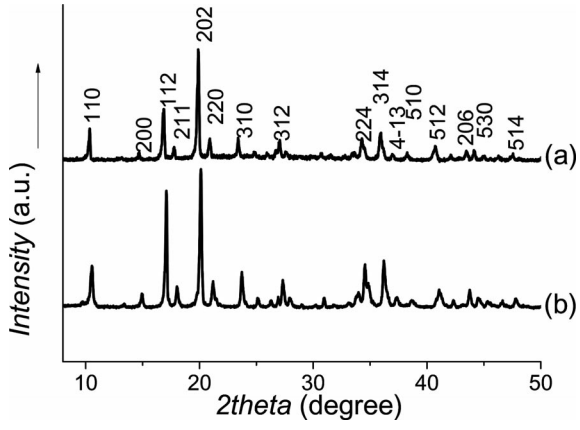

Figure 1. XRD patterns of (a) the $Mn_2W(CN)_8{\cdot}xH_2O$ product prepared at 65 °C and (b) the standard pattern of $Mn_2W(CN)_8{\cdot}xH_2O$.

Figure 2 shows scanning electron microscopy (SEM) images of the sample, from which it can be clearly seen that the sample is composed of a great number of uniform square microplatelets. These microplatelets have sharp edges, smooth surface and regular shape; they have an average size of 3 μm. The thickness was determined to be about 600 nm. Possibly owing to the higher content of organic groups (-CN) in the sample, it was difficult to study this material by using transmission electron microscopy because of rapid decomposition under irradiation with the electron beam. Considering the tetragonal phase crystal structure of $Mn_2W(CN)_8{\cdot}xH_2O$, it is proposed that the square microplatelets are mainly covered with {001} lattice planes. The FTIR spectrum of the sample (see the Supporting Information, Figure S1) shows a strong peak at 2123 cm^{-1} attributed to the C≡N stretching vibration, and two peaks at around 1620 and 3419 cm^{-1} ascribed to the C=O stretching of the PVP amide unit and O–H stretching of H_2O, respectively. This suggests that PVP molecules are adsorbed on the surface of $Mn_2W(CN)_8{\cdot}xH_2O$ crystals and crystal water exists in the as-synthesized products.

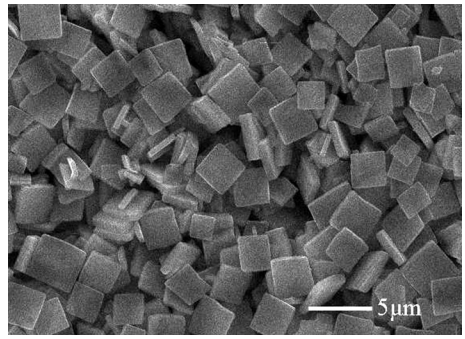

Figure 2. SEM image of $Mn_2W(CN)_8{\cdot}xH_2O$ microplatelets prepared at 65 °C.

Effects of Reaction Temperature

It was found that the reaction temperature has an important influence on the size and morphology of $Mn_2W(CN)_8{\cdot}xH_2O$ microcrystals. XRD results revealed that samples prepared under a reaction temperature of 5–85 °C are $Mn_2W(CN)_8{\cdot}xH_2O$ phase, but when the reaction temperature was increased to 95 °C, material with unidentified composition instead of $Mn_2W(CN)_8{\cdot}xH_2O$ was formed, suggesting that a reaction temperature of 95 °C (or higher) is not suitable for the synthesis of $Mn_2W(CN)_8{\cdot}xH_2O$ by using this route (see the Supporting Information, Figure S2). Samples prepared with different temperatures generated the same FTIR spectra (see the Supporting Information, Figure S1). Figure 3 shows SEM images of $Mn_2W(CN)_8{\cdot}xH_2O$ microcrystals synthesized in the temperature range 5–85 °C. As the temperature was gradually increased, the morphologies evolved sequentially from rice-like, rod-like, octahedron, square platelet, to hollow-cored square platelet. When the reaction temperature was lower than 15 °C, rice- and rod-like microcrystals were synthesized and the size of the rod-like microcrystals located at 7–23 μm in length and 1–4 μm in width (Figure 3, b). When the reaction temperature was raised to 20 °C, octahedral-like particles were formed with the coexistence of some rod-like particles (Figure 3, c). Regular octahedral particles with a size of ca. 2.5 μm were obtained at 25 °C.

Usually, crystal shape is determined by the growth rates of different crystal facets. When the crystal grows, the crystal gradually becomes surrounded by the facets of slower

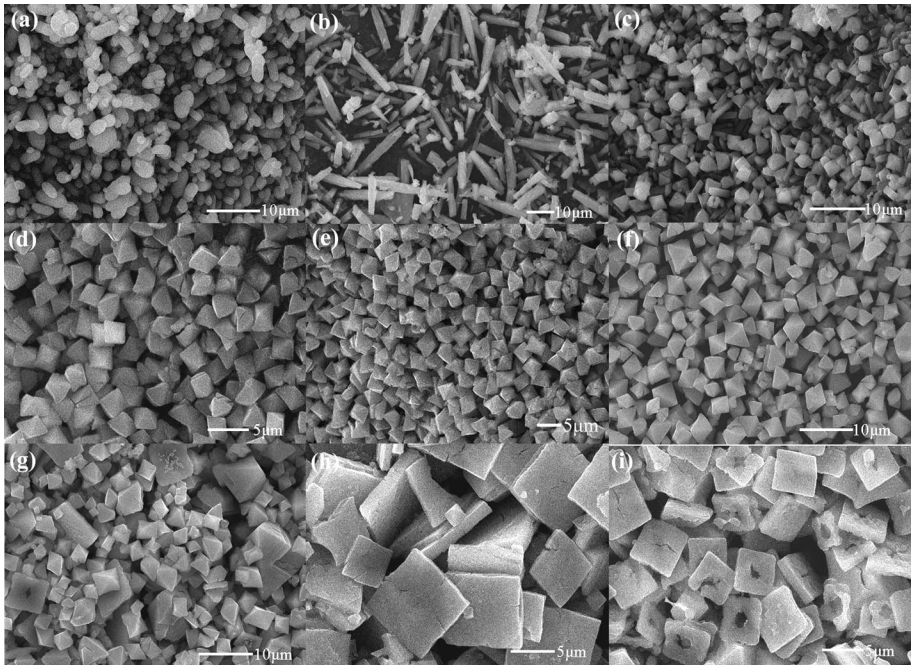

Figure 3. SEM images of $Mn_2W(CN)_8 \cdot xH_2O$ microcrystals with different morphologies obtained under different temperatures: (a) 5, (b) 15, (c) 20, (d) 25, (e) 35, (f) 45, (g) 55, (h) 75, (i) 85 °C.

growth. An octahedron is often surrounded by eight triangle facets of {111} in a tetragonal system. The experiments indicated that a temperature ranging from 25 to 55 °C is an appropriate region for the synthesis of octahedral microcrystals, whereas the sizes of the as-synthesized products were 3.6, 5.0, and 6.5 μm for temperatures of 35, 45, and 55 °C, respectively. Some square platelets were formed at 55 °C (Figure 3, g). With the reaction temperature up to 65 °C, well-defined square platelets were obtained (Figure 2). A temperature range of 65–75 °C seems to be an appropriate temperature region for the synthesis of square platelets, although their size increased from 3.0 to 9.6 μm (Figure 3, h) when the temperature was changed from 65 to 75 °C. Clearly, the size of the microcrystals increases with increasing reaction temperature. This is in accordance with the description of octahedral particles mentioned above. Products with hollow-cored square platelet morphology were generated at 85 °C (Figure 3, i). Thus, it can be concluded that temperatures of 20, 65, and 85 °C were the three key points for morphological transformation of $Mn_2W(CN)_8 \cdot xH_2O$ products.

Effects of Surfactant PVP

In a solution-phase synthesis, organic additives acting as surfactant or capping agent can change the order of free energies of different crystal facets through their interaction with metal sites on the surface.[32] PVP has been widely used in the synthesis of various microcrystals with rich morphologies and structures. For the synthesis of CP microcrystals, PVP is also a preferred additive owing to its nonionic bonding feature. In our case, the size and morphology of $Mn_2W(CN)_8 \cdot xH_2O$ microcrystals can also be tuned by changing the PVP concentration. XRD and IR spectra indicate that the samples prepared with different PVP concentrations are $Mn_2W(CN)_8 \cdot xH_2O$ (see the Supporting Information, Figure S3 and S4). Figure 4 shows the result of control experiments with different PVP concentrations at 25 °C. It can be seen that the morphologies of the particles change from octahedron to hollow-cored square platelet with increasing PVP concentration. When the concentration of PVP was low ([pyr]/[Mn^{2+}] = 50), the obtained $Mn_2W(CN)_8 \cdot xH_2O$ product was composed of irregular particles (Figure 4, a). When the ratio of [pyr]/[Mn^{2+}] was increased to 70, some octahedral microcrystals were formed

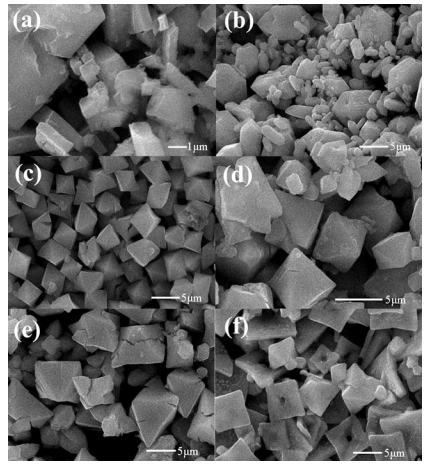

Figure 4. $Mn_2W(CN)_8 \cdot xH_2O$ microcrystals synthesized at 25 °C with different ratios of [pyr]/[Mn^{2+}]: (a) 50, (b) 70, (c) 100, (d) 120, (e) 150, and (f) 180.

among the irregular particles (Figure 4, b). Upon increasing PVP concentration up to [pyr]/[Mn^{2+}] = 100, large-scale octahedral microcrystals were obtained with a narrow size-distribution (Figure 3, d and c). There was no clear change of the morphology when the [pyr]/[Mn^{2+}] ratio was changed from 120 to 150, but the size of the particles increased from 5.8 to 9.5 μm (Figure 4, d and e). With [pyr]/[Mn^{2+}] = 180, some hollow-cored square platelets were obtained.

It is proposed that PVP plays a capping role for the shape tunable synthesis of $Mn_2W(CN)_8{\cdot}xH_2O$. With a certain concentration, PVP molecules would selectively bond on some crystal planes of the CP, inducing the formation of octahedral particles. It is well-documented that the viscosity of the solution has a significant function for crystal growth because it can affect the growth rate. To some extent, higher viscosity can slow down the nucleation and growth rate, and be more advantageous for fewer nuclei.[18] When the concentration of PVP is higher, the solution will have a higher viscosity. This would hinder the nucleation process, reducing the amount of crystal nuclei available, so increasing the size.[33] This is shown in Figure 4 (c–e), by increasing microcrystal size with increasing concentration of PVP. However, when the concentration of PVP was too high, the bonding of PVP on the surface of $Mn_2W(CN)_8{\cdot}xH_2O$ crystals would not be selective. In this situation, the particles show intrinsic square platelet shape as a result of its tetragonal crystal structure (Figure 4, f). It seems that the molecular weight of PVP also has an influence on the morphology of $Mn_2W(CN)_8{\cdot}xH_2O$ microcrystals. When smaller PVP was employed for the preparation, under otherwise identical conditions used to obtain microcrystals depicted in Figure 4 (c), rod-bundle or rod-like microcrystals were obtained (see the Supporting Information, Figures S5 and S6). Replacing the surfactant by polyethylene glycol (PEG) caused the formation of star-like structures, whereas with hexadecyltrimethy ammonium bromide (CTAB) as the surfactant, only irregular structures were obtained (see the Supporting Information, Figures S5 and S6). These results indicate that the surfactants have an important but complex influence on the morphology of $Mn_2W(CN)_8{\cdot}xH_2O$ microcrystals, which presumably originate from the multifarious interactions between the surfactant and coordination compound.

We also investigated the influence of the reactant (Mn^{2+}) concentration on the morphologies of $Mn_2W(CN)_8{\cdot}xH_2O$ microcrystals. Control experiments were performed by changing $MnSO_4$ concentration from 5 to 1 or 10 mM while keeping the other conditions the same as those for the octahedron product (Figure 3, d). It was found that 5 mM $MnSO_4$ was the optimum concentration for preparing $Mn_2W(CN)_8{\cdot}xH_2O$ microcrystals with regular shape and uniform size. With higher or lower $MnSO_4$ concentration, the particles were less uniform in shape and size.

Effects of Reaction Time

Figure 5 shows the morphological evolution of $Mn_2W(CN)_8{\cdot}xH_2O$ microcrystals with increasing reaction time at a reaction temperature of 25 °C. The corresponding XRD and IR results suggest that samples prepared with all reaction times are $Mn_2W(CN)_8{\cdot}xH_2O$ (see the Supporting Information, Figures S3 and S4). With 30 min reaction, only irregular $Mn_2W(CN)_8{\cdot}xH_2O$ crystals were obtained (Figure 5, a), whereas octahedrons were generated when the reaction time was increased to 60 min (Figure 5, b). Splits started to appear in the octahedral particles at reaction time of 90 min (Figure 5, c). Regular peanut-shaped particles then dominated at 120 min (Figure 5, d). When the reaction time was increased to 150 min, the crystals fully developed into rod-like crystals, and no peanut-like structures were observed at this reaction stage (Figure 5, e). Compared with the peanut-like particles, these rod-like particles have a clearly increased length and decreased diameter. In addition, the rod-like particles are not free-standing but twisted together with two, four, and even six intertwined together. Furthermore, branched particles were obtained when the reaction time reached 180 min (Figure 5, f). Therefore, the morphologies of $Mn_2W(CN)_8{\cdot}xH_2O$ microcrystals evolve from octahedron to peanut-like, rod-like, and branched particles with increasing reaction time. It is quite difficult to understand this morphological evolution process, which may relate to an Oswald ripening process as well as to the coordination interactions in the reaction system. With longer reaction time and continuous stirring, some particles dissolved, while some continued to grow, forming relatively stable structures.

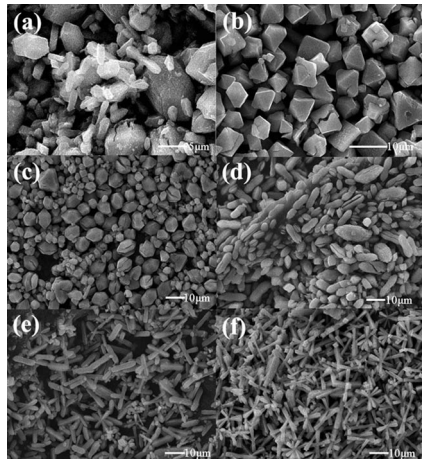

Figure 5. SEM images of $Mn_2W(CN)_8{\cdot}xH_2O$ microcrystals synthesized at 25 °C with various reaction times: (a) 30, (b) 60, (c) 90, (d) 120, (e) 150, (f) 180 min.

Growth Mechanism

Crystal growth is a very complex process. Shapes of microcrystals depend mainly on the intrinsic crystal structure of the materials, but are also strongly affected by reaction conditions such as reaction temperature, time, and additives.[34] Compared with those of inorganic compounds, surfactants have a more complex influence on the formation of coordination polymer micro/nanostructures due to the

more multifarious interactions operating between them. Our approach to the synthesis of microscale $Mn_2W(CN)_8{\cdot}xH_2O$ is to simply mix aqueous solutions of $W(CN)_8^{2-}$ and Mn^{2+} in the presence of PVP. Before the reaction, the Mn^{2+} ions are surrounded by PVP molecules. When $W(CN)_8^{2-}$ is added to the reaction system, the CN^- groups coordinate to Mn^{2+}, forming the $Mn_2W(CN)_8$ monomer at the initial nucleation stage. The presence of PVP slows down the nucleation and subsequent crystal growth. When the reaction temperature was below 20 °C, the precipitation process would be more rapid owing to the reduced solubility of the CP at lower temperature, which would cause the crystal to grow into one-dimensional structures with rice- or rod-like shape (Figure 3, a and b). When the temperature was increased to 25–45 °C, we consider that the intrinsic crystal features and the selective bonding of PVP on their crystal planes play dominant roles in the formation of the octahedral particles (Figure 3, d–f). When the temperature reached 65 °C, the bonding action of PVP would be weak, and the formation of $Mn_2W(CN)_8{\cdot}xH_2O$ tended to be low due to the higher solubility of the CP at higher temperature. Thus, square platelet particles, with their stable crystal shape reflecting the tetragonal structure, were obtained (Figure 2). Further increasing the temperature to 85 °C led to dissolution processes. It seems that the dissolution behavior of these $Mn_2W(CN)_8{\cdot}xH_2O$ microcrystals initiates at the center of square platelets, as evidenced by the formation of hollow-cored square particles (Figure 3, i).

Conclusions

By using a simple solution approach, $Mn_2W(CN)_8{\cdot}xH_2O$ microcrystals with various shapes and sizes were successfully prepared. The procedure involves the use of PVP to modify the growth behavior of CP. Various experimental parameters such as the reaction temperature, the feed ratio of Mn^{2+} to PVP, reaction time, and reactant concentration were systematically studied to delineate their influence on the shape and size of the $Mn_2W(CN)_8{\cdot}xH_2O$ products. It is believed that the obtained $Mn_2W(CN)_8{\cdot}xH_2O$ products have potential applications in molecular devices and gas storage. The shape and size controllable syntheses of $Mn_2W(CN)_8{\cdot}xH_2O$ crystals also shed some light on the fabrication of other octacyanometalate-based CPs.

Experimental Section

Preparation: Polyvinylpyrrolidone (PVP, K-30, average Mw = 40,000; K-25, average Mw = 24,000; K-17, average Mw = 8000), polyethylene glycol (PEG, average Mw = 1000), hexadecyltrimethy ammonium bromide (CTAB), $MnSO_4{\cdot}H_2O$, and other reagents were of analytical grade, purchased from Sinopharm Chemical Reagent Co. Ltd., and used without further purification. Double distilled water was used in all experiments. $K_4W(CN)_8{\cdot}2H_2O$ was prepared according to the literature.[35]

In a typical preparation of $Mn_2W(CN)_8{\cdot}xH_2O$ microcrystals, 20 mL of aqueous solution containing $MnSO_4{\cdot}H_2O$ (5 mM) and PVP was first prepared with $[pyr]/[Mn^{2+}] = 100$ (where pyr = pyrrolidone monomer). An aqueous solution of $K_4W(CN)_8{\cdot}2H_2O$ (5 mM, 10 mL) was added, which resulted in an immediate color change from deep-yellow to light-yellow. The mixture was stirred for 1 h at a specified temperature (5–85 °C), then two volumes of acetone was added to precipitate the CP products. The precipitate was collected by centrifugation, washed several times with absolute ethanol, then redispersed in ethanol for use.

Characterizations: The phase of the as-synthesized products was characterized by X-ray diffraction (XRD, Bruker D8 Advance diffractometer) with Cu-K_α radiation (λ = 1.5406 Å) at a scanning rate of 4°min^{-1}. X-ray tubes were operated with a current of 30 mA and voltage of 40 kV. The morphology and size of the obtained products were characterized by scanning electron microscopy (SEM, JSM-6480) and field emission scanning electron microscopy (FESEM, JSM-7001F). Fourier transform infrared (FTIR) spectra were recorded with a Nicolet Nexus 470 spectrometer with KBr pellets in the 4000–400 cm^{-1} region.

Supporting Information (see footnote on the first page of this article): XRD patterns, IR spectra, and selected SEM and TEM images.

Acknowledgments

The authors are grateful for financial support from the National Natural Science Foundation of China (NSFC) (grant numbers 51272094, 51072071 and 51102117) and the Specialized Research Fund for the Doctoral Program of Higher Education of China (grant number 20123227110018).

[1] A. P. Alivisatos, *Science* **1996**, *271*, 933–937.
[2] Y. Ding, S. H. Yu, C. Liu, Z. A. Zang, *Chem. Eur. J.* **2007**, *13*, 746–753.
[3] J. Hu, T. W. Odom, C. M. Lieber, *Acc. Chem. Res.* **1999**, *32*, 435–445.
[4] G. Markovich, C. P. Collier, S. E. Henrichs, F. Remacle, R. D. Levine, J. R. Heath, *Acc. Chem. Res.* **1999**, *32*, 415–423.
[5] A. M. Spokoyny, D. Kim, A. Sumrein, C. A. Mirkin, *Chem. Soc. Rev.* **2009**, *38*, 1218–1227.
[6] A. Carne, C. Carbonell, I. Imaz, D. Maspoch, *Chem. Soc. Rev.* **2011**, *40*, 291–305.
[7] R. Kaminker, R. Popovitz-Biro, M. E. Boom, *Angew. Chem.* **2011**, *123*, 3282; *Angew. Chem. Int. Ed.* **2011**, *50*, 3224–3226.
[8] T. Uemura, S. Kitagawa, *J. Am. Chem. Soc.* **2003**, *125*, 7814–7815.
[9] S. Vaucher, M. Li, S. Mann, *Angew. Chem.* **2000**, *112*, 1863; *Angew. Chem. Int. Ed.* **2000**, *39*, 1793–1796.
[10] M. Yamada, M. Arai, M. Kurihara, M. Sakamoto, M. Miyake, *J. Am. Chem. Soc.* **2004**, *126*, 9482–9483.
[11] A. Johansson, E. Widenkvist, J. Lu, M. Boman, U. Jansson, *Nano Lett.* **2005**, *5*, 1603–1606.
[12] J. Larionova, Y. Guari, C. Sangregoriob, C. Guérina, *New J. Chem.* **2009**, *33*, 1177–1190.
[13] L. Catala, D. Brinzei, Y. Prado, A. Gloter, O. Stéphan, G. Rogez, T. Mallah, *Angew. Chem. Int. Ed.* **2009**, *121*, 189–193.
[14] Y. Prado, L. Lisnard, D. Heurtaux, G. Rogez, A. Gloter, O. Stéphan, N. Dia, E. Rivière, L. Catala, T. Mallah, *Chem. Commun.* **2011**, *47*, 1051–1053.
[15] L. Hu, P. Zhang, Q. W. Chen, *Dalton Trans.* **2011**, *40*, 5557–5562.
[16] L. Hu, J. Y. Mei, Q. W. Chen, P. Zhang, N. Yan, *Nanoscale* **2011**, *3*, 4270–4274.
[17] L. Hu, J. Y. Mei, Q. W. Chen, J. Y. Mei, N. Yan, *RSC Adv.* **2011**, *1*, 1574–1578.

[18] L. Hu, P. Zhang, Q. W. Chen, H. Zhong, X. Y. Hu, X. R. Zheng, Y. Wang, N. Yan, *Cryst. Growth Des.* **2012**, *12*, 2257–2264.
[19] M. Clemente-León, E. Coronado, Á. López-Muñoz, D. Repetto, L. Catala, T. Mallah, *Langmuir* **2012**, *28*, 4525–4533.
[20] A. Tokarev, P. Agulhon, J. Long, F. Quignard, M. Robitzer, R. A. S. Ferreira, L. D. Carlos, J. Larionova, C. Guérina, Y. Guaria, *J. Mater. Chem.* **2012**, *22*, 20232–20242.
[21] R. Mouawia, J. Larionova, Y. Guari, S. Oh, P. Cook, E. Prouzet, *New J. Chem.* **2009**, *33*, 2449–2456.
[22] E. Coronado1, A. Forment-Aliaga1, E. Pinilla-Cienfuegos, S. Tatay, L. Catala, J. A. Plaza, *Adv. Funct. Mater.* **2012**, *22*, 3625–3633.
[23] S. Vaucher, J. Fielden, M. Li, E. Dujardin, S. Mann, *Nano Lett.* **2002**, *2*, 225–229.
[24] H. L. Sun, H. T. Shi, F. Zhao, L. M. Qi, S. Gao, *Chem. Commun.* **2005**, *34*, 4339–4340.
[25] M. Taguchi, I. Yagi, M. Nakagawa, T. Iyoda, Y. Einaga, *J. Am. Chem. Soc.* **2006**, *128*, 10978–10982.
[26] D. Brinzei, L. Catala, C. Mathoniere, W. Wernsdorfer, A. Gloter, O. Stephan, T. Mallah, *J. Am. Chem. Soc.* **2007**, *129*, 3778–3779.
[27] Y. Q. Mao, J. R. Chen, X. H. Wu, J. G. Miao, *Colloids Surf. A* **2007**, *295*, 135–138.
[28] G. L. Fu, W. Liu, S. S. Feng, X. L. Yue, *Chem. Commun.* **2012**, *48*, 11567–11569.
[29] L. Catala, C. Mathonière, A. Gloter, O. Stephan, T. Gacoin, J.-P. Boilot, T. Mallah, *Chem. Commun.* **2005**, 746–748.
[30] S. Brossard, F. Volatron, L. Lisnard, M. Arrio, L. Catala, C. Mathonière, T. Mallah, C. C. Moulin, A. Rogalev, F. Wilhelm, A. Smekhova, P. Sainctavit, *J. Am. Chem. Soc.* **2012**, *134*, 222–228.
[31] J. G. Leipoldt, L. D. C. Bok, P. J. Cilliers, *Z. Anorg. Allg. Chem.* **1974**, *407*, 350–352.
[32] Z. H. Xu, X. J. Kang, C. X. Li, Z. Y. Hou, C. M. Zhang, D. M. Yang, G. G. Li, J. Lin, *Inorg. Chem.* **2010**, *49*, 6706–6715.
[33] T. Uemura, Y. Hoshino, S. Kitagawa, K. Yoshida, S. Isoda, *Chem. Mater.* **2006**, *18*, 992–995.
[34] K. Liu, H. P. You, G. Jia, Y. H. Zheng, Y. J. Huang, Y. H. Song, M. Yang, L. H. Zhang, H. J. Zhang, *Cryst. Growth Des.* **2010**, *10*, 790–797.
[35] W. Dong, Y. Q. Sun, L. N. Zhu, D. Z. Liao, Z. H. Jiang, S. P. Yan, P. Cheng, *New J. Chem.* **2003**, *27*, 1760–1764.

Received: May 26, 2013
Published Online: September 9, 2013

